AJNR

Iterative Denoising Accelerated 3D FLAIR Sequence for Hydrops MR Imaging at 3T

R. Quint, A. Vaussy, A. Stemmer, C. Hautefort, E. Houdart and M. Eliezer

AJNR Am J Neuroradiol published online 3 August 2023
http://www.ajnr.org/content/early/2023/08/03/ajnr.A7953

Published August 3, 2023 as 10.3174/ajnr.A7953

Iterative Denoising Accelerated 3D FLAIR Sequence for Hydrops MR Imaging at 3T

R. Quint, A. Vaussy, A. Stemmer, C. Hautefort, E. Houdart, and M. Eliezer

ABSTRACT

BACKGROUND AND PURPOSE: 3D FLAIR sequences have become the criterion standard for identifying endolymphatic hydrops, but scan time remains an important limitation to their widespread use. Our purpose was to evaluate the diagnostic performance and image quality of an accelerated 3D FLAIR sequence combined with an iterative denoising algorithm.

MATERIALS AND METHODS: This was a retrospective study performed on 30 patients with clinical suspicion of endolymphatic hydrops who underwent 3T MR imaging 4 hours after gadolinium injection using two 3D FLAIR sequences. The first (conventional FLAIR) was accelerated with a conventional turbo factor of 187. The second was accelerated with an increased turbo factor of 263, resulting in a 33% scan time reduction (5 minutes 36 seconds versus 8 minutes 15 seconds, respectively). A sequence was reconstructed in-line immediately after the accelerated 3D FLAIR acquisition from the same raw data with iterative denoising (accelerated-FLAIR iterative denoising). The signal intensity ratio image quality score and endolymphatic hydrops diagnosis were evaluated.

RESULTS: The mean signal intensity ratio for symptomatic and asymptomatic ears of accelerated-FLAIR iterative denoising was significantly higher than the mean SNR of conventional FLAIR (29.5 versus 19 and 25.9 versus 16.3, $P < .001$). Compared with the conventional FLAIR sequence, the image-quality score was higher with accelerated-FLAIR iterative denoising (mean image-quality score, 3.8 [SD, 0.4] versus 3.3 [SD, 0.6] for accelerated-FLAIR iterative denoising and conventional FLAIR, respectively, $P = .003$). There was no significant difference in the diagnosis of endolymphatic hydrops between the 2 sequences. Interreader agreement was good-to-excellent.

CONCLUSIONS: The iterative denoising algorithm applied to an accelerated 3D FLAIR sequence for exploration of endolymphatic hydrops enabled significantly reducing the scan time without compromising image quality and diagnostic performance.

ABBREVIATIONS: acc = accelerated; conv = conventional; CS = compressed sensing; DLR = deep learning reconstruction; EH = endolymphatic hydrops; GRAPPA = generalized autocalibrating partially parallel acquisition; ID = iterative denoising; PI = parallel imaging; SIR = signal intensity ratio

Since the first MR imaging study performed by Nakashima et al,[1] in 2007, 3D FLAIR sequences performed 4 hours after IV contrast administration have become the criterion standard in clinical practice for identifying endolymphatic hydrops (EH) in patients with suspicion of Menière disease and other inner ear disorders.[2-4]

Despite the significantly increased quality of these high-resolution sequences, the scan time is an important limitation to the widespread use of the hydrops protocol, with acquisition lengths up to 15 minutes in some centers.

Received February 13, 2023; accepted after revision June 27.

From the Departments of Neuroradiology (R.Q., E.H., M.E.), and Head and Neck Surgery (C.H.), Lariboisière University Hospital, Paris, France; Siemens Healthineers France (A.V.), Saint-Denis, France; Siemens Healthineers (A.S.), Erlangen, Germany; and Faculté de Médecine (E.H.), Université de Paris, Paris, France.

Please address correspondence to Michael Eliezer, MD, Department of Neuroradiology, Lariboisière University Hospital, 75010 Paris, France; e-mail: michael.eliezer@aphp.fr

http://dx.doi.org/10.3174/ajnr.A7953

Parallel imaging (PI) acceleration techniques, based on phased array coils, are used to significantly decrease scan time, improving patient comfort, image quality, and cost-effectiveness.[5] Sensitivity encoding and generalized autocalibrating partially parallel acquisition (GRAPPA) are the most commonly used techniques for clinical MR imaging systems.[6,7] However, by increasing the acceleration factor, the reduction of the acquisition time is limited by a significant SNR loss.

Although variable flip angle sequences are frequently used because they allow keeping the high-signal amplitude during a long readout duration,[8] it has been demonstrated that 3D FLAIR sequences with a constant flip angle provide a higher signal and contrast intensity ratio for EH evaluation.[9] Nevertheless, the use of constant flip angle sequences with a high echo-train length can compromise the SNR, compensated for by an extended scan time.

Recently, Naganawa et al[10] reported a 5-minute HYDROPS2-Mi2 sequence by increasing the PI factor and decreasing the

Table 1: Imaging parameters for 3D FLAIR EH MR imaging sequences

	Conv-FLAIR	Acc-FLAIR-ID
FOV (frequency × phase) (mm^2)	154 × 154	154 × 154
Matrix	256 × 256	256 × 256
Orientation	Axial	Axial
Section thickness (mm)	0.8	0.8
GRAPPA	2	2
No. of slices	28	28
TR/TE/TI (ms)	16,000/640/3000	16,000/640/3000
Flip angle	Constant 140°	Constant 140°
Turbo factor	187	263
Bandwidth (Hz/pixel)	279	501
Scanning time	8 minutes 15 seconds	5 minutes 36 seconds

acquisition coverage with a reduced number of slices. The signal loss was compensated for by using a deep learning reconstruction (DLR) algorithm.[11]

Another approach using an iterative denoising (ID) reconstruction algorithm, which works with quantitative noise information, has been proposed to compensate for the SNR loss penalty inherent in the high acceleration factor. This strategy has been evaluated for MR imaging of various organs, and these studies highlighted a significantly decreased scan time while preserving image quality and SNR.[12-14]

This study aimed to evaluate the diagnostic performance and image quality of an accelerated 3D FLAIR sequence with ID reconstruction for EH exploration at 3T.

MATERIALS AND METHODS

Study Design

This single-center retrospective study was approved by our institutional Research Ethics Board (NTC 02529475) and adhered to the tenets of the Declaration of Helsinki. Informed consent was waived. This study follows the Strengthening Reporting of Observational Studies in Epidemiology (STROBE) guidelines. The on-site institutional PACS and electronic patient medical records of our center were queried from October 2020 and May 2021, to identify patients referred for "hydrops protocol" MR imaging. A total of 924 patients with a hydrops MR imaging protocol were evaluated for inclusion.

The medical charts of all patients were systematically reviewed by 1 otoneurologist (C.H.). Demographic features were recorded as well as clinical reports including detailed neuro-otologic examinations.

Patients

Among the 924 patients, 30 patients (60 ears) had undergone both a conventional 3D FLAIR (conv-FLAIR) and an accelerated 3D FLAIR with ID (acc-FLAIR-ID) during the implementation of this sequence in our center. These patients had various cochleovestibular symptoms and a clinical suspicion of EH after evaluation by an otolaryngologist (C.H.).

MR Imaging Protocol

MR imaging examinations were performed on a 3T Magnetom Skyra (Siemens) scanner with a Head/Neck 64 coil (Siemens). All patients underwent MR imaging 4 hours after a single IV dose of gadobutrol (Gd-DO3A-butrol; Gadovist, 0.1 mmol/kg, 1 mmol/mL; Bayer Schering Pharma) that provided a high contrast in the labyrinth.[15]

All patients underwent heavily T2-weighted sequences for an anatomic reference of the labyrinthine fluid, as well as diffusion-weighted and 3D FLAIR sequences of the brain.

Two 3D FLAIR sequences were successively performed for each patient. Detailed scan parameters are summarized in Table 1.

The first acquisition, conv-FLAIR, was accelerated with a conventional GRAPPA factor of 2 and a turbo factor of 187, as used in the clinical routine at our institution. The second acquisition was also accelerated with an increased turbo factor of 263, while the GRAPPA factor was maintained at 2, resulting in a 33% scan-time reduction (5 minutes 36 seconds versus 8 minutes 15 seconds, respectively). To maintain the same echo-train length (1212 ms), we increased the bandwidth (501 versus 279 Hz/pixel), resulting in a 25% SNR loss. A sequence was reconstructed in-line immediately after the accelerated 3D FLAIR acquisition from the same raw data with ID (acc-FLAIR-ID).

Iterative Denoising

The ID prototype algorithm was integrated into the reconstruction pipeline of the MR imaging scanner. Data processing was performed in-line using the ID algorithm. Patient-specific noise maps were measured using the adjustment framework of the system, ensuring a precise estimation of the heterogeneous noise distribution. An additional edge enhancement was built into the ID processing, which would undo some of the SNR improvement while producing a sharper image appearance. A denoising strength of 110% was chosen to efficiently reduce the noise while maintaining a detailed level of fine anatomic structures.

Imaging Analysis

For each patient, MR images were evaluated with Carestream Vue 12.1 (Philips Healthcare) by 1 neuroradiologist (M.E.) with 7 years of experience in inner ear imaging and 1 radiology resident (R.Q.) blinded to the clinical data and to the acquisition scheme of the different data sets.

For each examination, 2 data sets were independently evaluated: 1) the conv-FLAIR, and 2) the acc-FLAIR-ID. All images were randomly interpreted.

Qualitative Assessment. Overall image quality was rated on a 4-point scale as follows: 1 = "poor:" limiting diagnostic capability; 2 = "fair:" not preventing diagnostic capability but significantly decreased image quality; 3 = "good:" minor artifacts; and 4 = "excellent:" no artifacts.

Quantitative Assessment. Quantitative assessment was performed with the ROI method.[16] For the signal intensity of the perilymphatic space, a 5-mm^2 circular ROI was placed in the basal turn of the cochlea. For the signal intensity of the noise, a 50-mm^2 circular ROI was placed at the same level in the medulla. The SNR, also known as signal intensity ratio (SIR), was defined as the signal

intensity of the basal turn divided by the SD of noise in the medulla (SIR = Siperilymph / SD of SInoise).

MR Imaging Evaluation. For the diagnosis of EH, we used the grading systems previously described in the literature,[17] as follows: 1) Cochlear hydrops was reported present in case of obstruction of the scala vestibuli by the endolymphatic space; 2) saccular hydrops was reported present when the saccule appeared larger than the utricule or touched the oval window; 3) utricular hydrops was defined when there was herniation of the utricle in part of the lateral semicircular canal or when there was no surrounding perilymphatic space.

Statistical Analysis. Data were analyzed using R statistical and computing software, Version 3.3.2 (http://www.r-project.org/). Comparison of the SIR between the conv-FLAIR and acc-FLAIR-ID sequences was assessed by a *t* test. Visual assessment between the conv-FLAIR and acc-FLAIR-ID sequences was compared using the Fisher exact test. To evaluate the reproducibility of the qualitative analysis, we calculated interreader agreement with the Cohen κ coefficient.[18] Continuous data were expressed as mean and SD. Categoric data were expressed as frequencies and percentages. Significance was set at $P < .05$.

Table 2: Qualitative assessment independently performed by 2 blinded radiologists on a 4-point scale[a]

	Conv-FLAIR		Acc-FLAIR-ID	
	Senior Radiologist	Junior Radiologist	Senior Radiologist	Junior Radiologist
Poor	0	5	0	5
Fair	3	4	0	2
Good	15	16	6	15
Excellent	12	5	24	8

[a] 1, poor; 2, fair; 3, good; and 4, excellent.

RESULTS

Population

Thirty patients (18 women and 12 men) with a mean age of 51.6 (SD, 16.6) years (range, 23–86 years) were included in this study. A total of 60 ears were analyzed.

MR Imaging Data

Quantitative Analysis. For conv-FLAIR, the mean SIR for the symptomatic and asymptomatic ears was 19 (SD, 8) and 16.3 (SD, 6.8), respectively. For acc-FLAIR-ID, the mean SIR for the symptomatic and asymptomatic ears was 29.5 (SD, 15.7) and 25.9 (SD, 10.5), respectively. The mean SIR for symptomatic and asymptomatic ears of acc-FLAIR-ID was significantly higher than the mean SNR of conv-FLAIR ($P < .001$).

Image-Quality Subjective Analysis. Pooled image quality scores are shown in Table 2.

For the senior radiologist, the mean overall image quality was considered good for conv-FLAIR (3.3 [SD, 0.6]) and acc-FLAIR-ID (3.8 [SD, 0.4]). For conv-FLAIR, image quality of 3 patients was rated as fair; 15 patients, as good; and 12 patients, as excellent. For acc-FLAIR-ID, image quality of 6 patients was rated as good, and 24 patients, as excellent. The improved image-quality score was significantly different for acc-FLAIR-ID compared with conv-FLAIR ($P = .003$) (Fig 1).

For the junior radiologist, the mean overall image quality was considered as good for conv-FLAIR (2.7 [SD, 1]) and acc-FLAIR-ID (2.8 [SD, 1]). For conv-FLAIR, image quality for 5 patients was rated as poor; 4 patients, as fair; 16 patients, as good; and 5 patients, as excellent. For acc-FLAIR-ID, image quality of 5 patients was rated as poor; 2 patients, as fair; 15 patients, as good; and 8 patients, as excellent. The image-quality score was not significantly different for acc-FLAIR-ID compared with conv-FLAIR ($P = .38$).

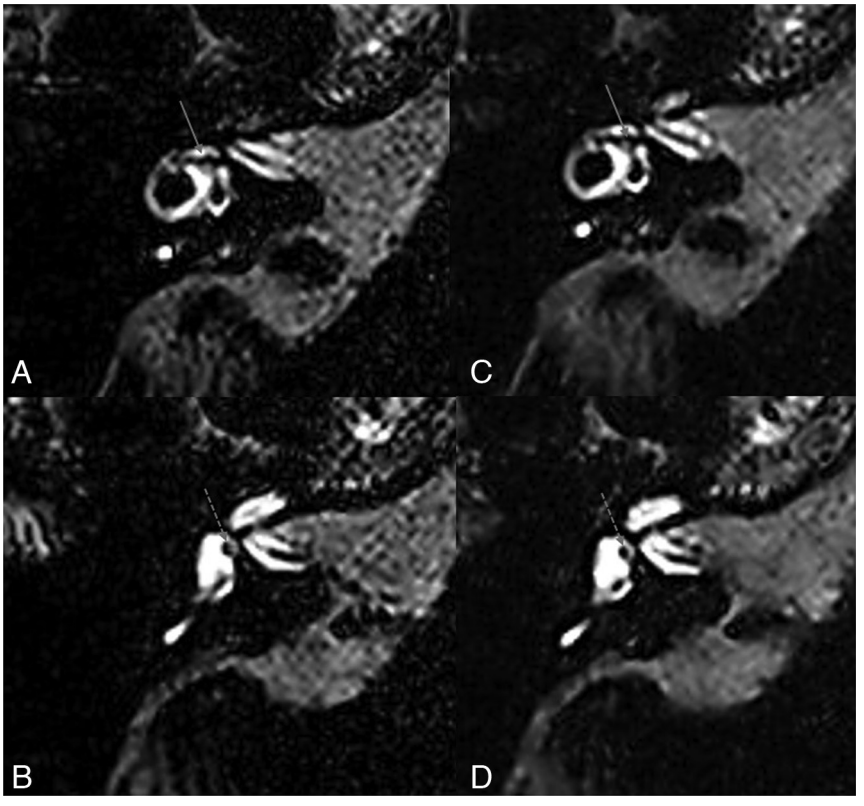

FIG 1. An example of conv-FLAIR (*A* and *B*) and acc-FLAIR-ID (*C* and *D*) images with normal findings in the same patient without hydrops. *A* and *C*, The level of the utricule (*white arrow*) and the lateral semicircular canal. *B* and *D*, The level of the saccule (*dashed white arrow*). Both sequences were rated as excellent. Note the sharper appearance of the acc-FLAIR-ID images, which were acquired with a 33% scan time reduction.

EH Evaluation

For conv-FLAIR, EH was observed in 18/60 ears (30%): cochlear hydrops ($n = 15$), saccular hydrops ($n = 18$), utricular hydrops ($n = 8$) by the senior

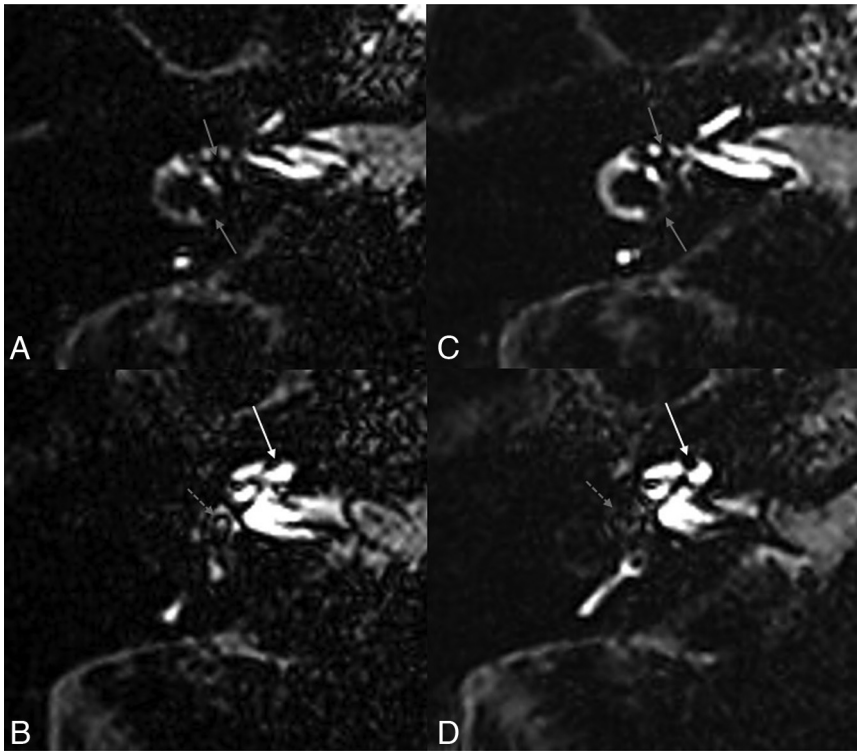

FIG 2. Conv-FLAIR (*A* and *B*) and Acc-FLAIR-ID (*C* and *D*) images of a patient with cochlear, saccular, and utricular hydrops. *A* and *C*, Utricular hydrops: an enlarged utricule (*white arrow*) with partial obstruction of the perilymphatic space and herniation in the posterior limb of the lateral semicircular canal. *B* and *D*, Cochlear and saccular hydrops: an enlarged endolymphatic space with obstruction of the scala vestibuli (*white arrow*) and an enlarged saccule (*dashed arrow*), confluent with the utricule from which it is not distinguishable.

Table 3: Pooled diagnostic assessment of hydrops independently performed by 2 blinded radiologists[a]

	Conv-FLAIR			Acc-FLAIR-ID		
	Senior	Junior	κ	Senior	Junior	κ
Cochlear hydrops	15/60	10/60	0.75 (0.57–0.93)	15/60	11/60	0.81 (0.65–0.96)
Saccular hydrops	18/60	12/60	0.74 (0.57–0.90)	18/60	13/60	0.81 (0.65–0.96)
Utricular hydrops	8/60	8/60	1 (1.00–1.00)	10/60	8/60	0.78 (0.63–0.94)

[a] There were no significant differences for all EH locations between the 2 sequences. The κ coefficients for interobserver agreement were good-to-excellent.

reader (Fig 2). For acc-FLAIR-ID, EH was also observed in 18/60 ears (30%): cochlear hydrops ($n = 15$), saccular hydrops ($n = 18$), utricular hydrops ($n = 10$) by the senior reader. There were no significant differences for all EH locations ($P < .001$) between the 2 sequences (Fig 2).

For conv-FLAIR, EH was observed in 12/60 ears (20%): cochlear hydrops ($n = 10$), saccular hydrops ($n = 12$), utricular hydrops ($n = 8$) by the junior reader (Fig 2). For acc-FLAIR-ID, EH was observed in 13/60 ears (21.7%): cochlear hydrops ($n = 11$), saccular hydrops ($n = 13$), utricular hydrops ($n = 8$) by the junior reader. There were no significant differences for all EH locations ($P < .001$) between the 2 sequences (Table 3).

With conv-FLAIR, the interreader agreement was good for cochlear (0.75 [0.57–0.93]) and saccular (0.74 [0.57–0.90]) hydrops and excellent (1 [1.00–1.00]) for utricular hydrops. With acc-FLAIR-ID, the interreader agreement was very good for cochlear (0.81 [0.65–0.96]) and utricular (0.81 [0.65–0.96]) hydrops, and good for saccular hydrops (0.78 [0.63–0.94]).

DISCUSSION

In this study, we demonstrated that an accelerated 3D FLAIR sequence combined with an ID algorithm enabled reducing the scan time by 33% without compromising image quality and diagnostic performance for EH. As expected, the SNR was significantly increased with acc-FLAIR-ID compared with conv-FLAIR because a noise-reduction algorithm was used.

An MR imaging evaluation of the endolymphatic space relies on the selective enhancement of the perilymphatic space after administration of IV contrast media, which enables distinguishing the endolymphatic and perilymphatic spaces.[1,3] The main limiting factor is the low concentration of gadolinium obtained in the perilymphatic space. To overcome this, we optimized several parameters to increase the signal intensity. First, the administration of gadolinium-based contrast agents with higher longitudinal relaxivity and concentration has been recommended.[15] Second, a constant flip angle instead of a variable flip angle provides higher signal and contrast in the perilymphatic space, by shortening the longitudinal relaxation induced by gadolinium.[9] However, the use of a constant flip angle with a high echo-train length compromises the SNR. Third, the signal intensity of the perilymphatic space increases using a long TR (16,000 ms), which allows sufficient longitudinal magnetization regrowth to detect minor T1-shortening related to low gadolinium concentration.[19,20] Yet, a long TR contributes to the long acquisition time, which is an important limitation to the wide spread of this protocol.

PI acceleration techniques, based on phased array coils, might be used to significantly decrease scan time to overcome the long acquisition time of these sequences. However, by increasing the acceleration factor, the reduction of the acquisition time is limited by a significant decrease in SNR (by a factor of the square root of the acceleration factor) because fewer data points are acquired and averaged.[5,21] In PI-reconstructed images, the SNR also depends on the spatially varying noise characteristics and amplification in the final images, quantified by the g-factor, which originates from the coil sensitivities. Because inner ear imaging requires reduced section acquisition coverage with activation of a few coil elements, the use of a higher acceleration

factor is limited. Moreover, PI techniques are particularly sensitive to motion artifacts that might occur between the time of the calibration scan and image acquisition. Thus, we have decided to increase the turbo factor and the receiver bandwidth instead of increasing the PI acceleration factor. 3D FLAIR sequences for EH exploration are less susceptible to signal loss due to the weaker later echoes affected by T2 decay. Indeed, inner ear imaging is particularly suitable for the use of a high turbo factor with a long echo-train because the T2 values of the labyrinthine fluid are high (similar to CSF, which is around 2000 ms at 3T). Despite the high turbo factor used, blurring is avoided because the echo-train duration remains inferior to 2–3 times the T2 values of the primary interest area.[8] By increasing the bandwidth, we were able to reduce interecho spacing to maintain the same readout time while increasing the number of echoes, decreasing the total scan time. Nevertheless, the inherent result of an increased bandwidth is a 25% SNR loss because of the amount of noise that is sampled due to the larger frequency range.

The ID algorithm compensated for the signal loss caused by using a constant flip angle with a long echo-train length and the increased bandwidth. Recently, Naganawa et al[10] achieved a 5-minute HYDROPS-Mi2 sequence with DLR. The reduction in acquisition time was mainly obtained by decreasing the number of slices (224 to 60), while the SNR loss was compensated for with the DLR. The DLR tool incorporates a deep convolutional neural network restoration process into the reconstruction flow and enables noise reduction. DLR is a nonlinear processing with behaviors potentially difficult to predict.[22] Thus, in our experience, ID allows better control of the denoising process, parameters, and strength, ensuring a precise estimation of the heterogeneous noise distribution.

Other acceleration approaches such as compressed sensing (CS) have been introduced to reduce the scan time. CS is based on incoherent subsampling of the Fourier space, transformation of the image into a sparse representation, and nonlinear iterative reconstruction.[23] It is used in various applications and is particularly suitable for indications in which images are sparse, such as MRA.[24] However, other applications with low sparsity, such as 3D morphologic sequences with high spatial resolution, offer little acceleration potential with CS. In addition, artifacts such as image blurring and global ringing have been described with CS, notably for MR neuroimaging,[25] which limits the acceleration rates achievable. CS is also limited by its extended reconstruction time, which can be reduced with the use of a graphic processing unit, though it is not available on all clinical MR imaging scanners.

Conversely, an ID algorithm can be performed on conventional computers without a significant increase of reconstruction time. The use of a quantitative noise map in ID is particularly suited to limit the g-factor penalty associated with high acceleration rates, as well as the SNR loss related to the increased bandwidth.

Our study has several limitations. EH was reported as present or absent by an anatomic system, but we did not use grading or volumetric assessment. However, our hydrops assessment was based on a previously reported anatomically-based grading system,[17] and the grading used should not have impacted diagnostic relevancy.

The use of a 3T system and a 64-channel phased array head coil contributed to the high image quality. The SNR improvement with ID could improve the image quality of 1.5T scanners, which are more available, and further studies should be performed at 1.5T or with lower head coil density.

Our study has several clinical implications. By reducing the scan time, patient comfort and satisfaction are increased, reducing the risk of motion artifacts. Shortening the imaging time will also allow a higher patient throughput and is expected to promote wider use of MR imaging for the evaluation of EH. In our institution, about 40 patients per week undergo inner ear MR imaging. A 33% scan time reduction of 8 minutes 15 seconds would allow 120 minutes of additional machine time.

Along with the scan time, the 4-hour delay after gadolinium injection contributes to the logistical strains of EH imaging. Our group showed in a recent work that with optimized 3D FLAIR parameters, the postinjection delay could be shortened to 2 hours with sufficient contrast for EH evaluation, which should further shorten the imaging time and promote a wider use of EH MR imaging.[26]

CONCLUSIONS

3D FLAIR sequences for EH evaluation require optimal parameters to obtain sufficient signal in the perilymphatic space. The trade-off and one of the main limitations are long acquisition times. In this study, the ID algorithm was successfully applied to an accelerated 3D FLAIR sequence for EH exploration with significantly reduced scan time without compromising image quality and the diagnostic performance.

Disclosure forms provided by the authors are available with the full text and PDF of this article at www.ajnr.org.

REFERENCES

1. Nakashima T, Naganawa S, Sugiura M, et al. **Visualization of endolymphatic hydrops in patients with Meniere's disease**. *Laryngoscope* 2007;117:415–20 CrossRef Medline
2. Eliezer M, Attyé A, Toupet M, et al. **Imaging of endolymphatic hydrops: a comprehensive update in primary and secondary hydropic ear disease**. *J Vestib Res* 2021;31:261–68 CrossRef Medline
3. Connor SE, Pai I. **Endolymphatic hydrops magnetic resonance imaging in Ménière's disease**. *Clin Radiol* 2021;76:76.e1–19 CrossRef Medline
4. Gürkov R. **Menière and friends: imaging and classification of hydropic ear disease**. *Otol Neurotol* 2017;38:e539–44 CrossRef Medline
5. Deshmane A, Gulani V, Griswold MA, et al. **Parallel MR imaging.** *J Magn Reson Imaging* 2012;36:55–72 CrossRef Medline
6. Pruessmann KP, Weiger M, Scheidegger MB, et al. **SENSE: sensitivity encoding for fast MRI.** *Magn Reson Med* 1999;42:952–62 Medline
7. Griswold MA, Jakob PM, Heidemann RM, et al. **Generalized autocalibrating partially parallel acquisitions (GRAPPA).** *Magn Reson Med* 2002;47:1202–10 CrossRef Medline
8. Mugler JP. **Optimized three-dimensional fast spin-echo MRI.** *J Magn Reson Imaging* 2014;39:745–67 CrossRef Medline
9. Nahmani S, Vaussy A, Hautefort C, et al. **Comparison of enhancement of the vestibular perilymph between variable and constant flip angle–delayed 3D FLAIR sequences in Menière disease**. *AJNR Am J Neuroradiol* 2020;41:706–11 CrossRef Medline
10. Naganawa S, Ito R, Kawai H, et al. **MR imaging of endolymphatic hydrops in five minutes.** *Magn Reson Med Sci* 2021;21:401–40 CrossRef Medline

11. Naganawa S, Nakamichi R, Ichikawa K, et al. **MR imaging of endolymphatic hydrops: utility of iHYDROPS-Mi2 combined with deep learning reconstruction denoising.** *Magn Reson Med Sci* 2021;20:272–79 CrossRef Medline
12. Eliezer M, Vaussy A, Toupin S, et al. **Iterative denoising accelerated 3D SPACE FLAIR sequence for brain MR imaging at 3T.** *Diagn Interv Imaging* 2022;103:13–20 CrossRef Medline
13. Almansour H, Weiland E, Kuehn B, et al. **Accelerated three-dimensional T2-weighted turbo-spin-echo sequences with inner-volume excitation and iterative denoising in the setting of pelvis MRI at 1.5T: impact on image quality and lesion detection.** *Acda Radiol* 2022;29:e248–59 CrossRef Medline
14. Kang HJ, Lee JM, Ahn SJ, et al. **Clinical feasibility of gadoxetic acid-enhanced isotropic high-resolution 3-dimensional magnetic resonance cholangiography using an iterative denoising algorithm for evaluation of the biliary anatomy of living liver donors.** *Invest Radiol* 2019;54:103–09 CrossRef Medline
15. Eliezer M, Poillon G, Gillibert A, et al. **Comparison of enhancement of the vestibular perilymph between gadoterate meglumine and gadobutrol at 3-Tesla in Meniere's disease**. *Diagn Interv Imaging* 2018;99:271–77 CrossRef Medline
16. Pakdaman MN, Ishiyama G, Ishiyama A, et al. **Blood-labyrinth barrier permeability in Menière disease and idiopathic sudden sensorineural hearing loss: findings on delayed postcontrast 3D-FLAIR MRI**. *AJNR Am J Neuroradiol* 2016;37:1903–08 CrossRef Medline
17. Kahn L, Hautefort C, Guichard JP, et al. **Relationship between video head impulse test, ocular and cervical vestibular evoked myogenic potentials, and compartmental magnetic resonance imaging classification in Menière's disease**. *Laryngoscope* 2020;130:E444–52 CrossRef Medline
18. Benchoufi M, Matzner-Lober E, Molinari N, et al. **Interobserver agreement issues in radiology.** *Diagn Interv Imaging* 2020;101:639–41 CrossRef Medline
19. Osman S, Hautefort C, Attyé A, et al. **Increased signal intensity with delayed post contrast 3D FLAIR MRI sequence using constant flip angle and long repetition time for inner ear evaluation**. *Diagn Interv Imaging* 2022;103:225–29 CrossRef Medline
20. Kato Y, Bokura K, Taoka T, et al. **Increased signal intensity of low-concentration gadolinium contrast agent by longer repetition time in heavily T2-weighted-3D FLAIR.** *Jpn J Radiol* 2019;37:431–35 CrossRef Medline
21. Robson PM, Grant AK, Madhuranthakam AJ, et al. **Comprehensive quantification of signal-to-noise ratio and g-factor for image-based and k-space-based parallel imaging reconstructions.** *Magn Reson Med* 2008;60:895–907 CrossRef Medline
22. Higaki T, Nakamura Y, Tatsugami F, et al. **Improvement of image quality at CT and MRI using deep learning.** *Jpn J Radiol* 2019;37:73–80 CrossRef Medline
23. Yang AC, Kretzler M, Sudarski S, et al. **Sparse reconstruction techniques in magnetic resonance imaging: methods, applications, and challenges to clinical adoption.** *Invest Radiol* 2016;51:349–64 CrossRef Medline
24. Lustig M, Donoho D, Pauly JM. **Sparse MRI: The application of compressed sensing for rapid MR imaging.** *Magn Reson Med* 2007;58:1182–95 CrossRef Medline
25. Sartoretti T, Reischauer C, Sartoretti E, et al. **Common artefacts encountered on images acquired with combined compressed sensing and SENSE.** *Insights Imaging* 2018;9:1107–15 CrossRef Medline
26. Barlet J, Vaussy A, Ejzenberg Y, et al. **Optimized 3D FLAIR sequences to shorten the delay between intravenous administration of gadolinium and MRI acquisition in patients with Menière's disease**. *Eur Radiol* 2022;32:6900–09 CrossRef Medline